IJLAI Transactions on Science and Engineering (ISSN: 3006-3418) 2025, vol. 3, no. 4, pp: 21–30

A Novel Clustering Feature-Based BiLSTM-GAN Method for Enhancing ECG Signal

Xibin Guo[1], Zhenyu Heng[1], and Jianwei Fang[1]

School of Electronics and Electrical Engineering, Zhengzhou University of Science and Technology
450064 Zhengzhou, China
Received Nov. 16, 2025; Revised and Accepted Nov. 20, 2025

Abstract. Electrocardiogram (ECG) signals are frequently corrupted by diverse noises that degrade the accuracy of downstream arrhythmia detection and hamper reliable tele-cardiology. This paper proposes a clustering feature-driven Bidirectional-LSTM Generative Adversarial Network (CF-BiLSTM-GAN) that learns to recover clean heartbeat morphology from single-channel, noisy recordings. First, an adaptive k-means module is employed on the latent space of a pre-trained denoising auto-encoder to discover representative beat-level clusters; these clusters are treated as high-level priors that encode patient-specific QRS-T shape constraints. Second, a BiLSTM generator conditioned on the cluster centroids is trained within a GAN framework to reconstruct the temporal manifold of the ECG while preserving subtle atrial/ventricular signatures. A spectral-normalized CNN discriminator enforces local smoothness and global periodicity, suppressing both high-frequency artifacts and baseline wander simultaneously. Experiments on MIT-BIH and PhysioNet/CinC datasets demonstrate that CF-BiLSTM-GAN outperforms state-of-the-art wavelet, dictionary-learning, and vanilla DL methods, achieving lower MSE, higher cross-correlation and improved beat classification F1 after denoising. The proposed approach offers a practical, data-driven solution for enhancing ECG fidelity in ambulatory monitoring and edge devices.

Keywords: ECG denoising; BiLSTM-GAN; clustering feature; heartbeat morphology.

1. Introduction

Cardiovascular diseases (CVDs) have always been the leading cause of sudden cardiac death worldwide. According to the data from the World Health Organization (WHO) in 2017, 17.9 million people die from cardiovascular diseases each year, accounting for 31% of the global death toll. Heart attacks and strokes account for 85% of these deaths. Studies have shown that 90% of heart attacks can be effectively prevented and diagnosed [1-3]. Electrocardiogram (ECG) is a mature diagnostic technique for heart diseases and can provide early and effective diagnosis, which is crucial for preventing heart attacks. ECG can assess the physiological condition of the heart and detect various abnormalities, such as arrhythmias and coronary artery blockages. ECG signals can be severely damaged during collection and transmission due to various noise interferences, making it difficult to extract useful morphological feature information from the electrocardiogram signals and interpret the electrocardiogram signals, thereby leading to unreliable or incorrect detection of heart diseases and hindering the discovery of heart diseases. The complex noise in ECG is mainly muscle electrical interference, baseline drift, electrode interference, and power frequency interference. Among them, power frequency interference is a fixed noise from the human electromagnetic field, generally a stable noise at a frequency of 50Hz, which is relatively easy to remove. Therefore, it is very important to accurately remove muscle electrical interference, baseline drift, and electrode interference noise from the electrocardiogram signals without losing useful information [4-6].

The collected electrocardiogram (ECG) signals contain complex noise. The goal of ECG signal denoising is not only to remove the complex noise, but also to retain as much useful signal information as possible. Since the frequencies of some ECG signals and noise overlap, this remains a challenging task. In recent years, there have been many studies on ECG signal denoising. Traditional denoising methods include wavelet-based algorithms [7-9], empirical mode decomposition (EMD) [10], and adaptive digital filters [11]. Among them, wavelet-based denoising algorithms eliminate noise by decomposing the signal in the time-frequency domain, and are the most widely used in ECG denoising. Wavelet coefficients can be processed using hard thresholding and soft thresholding. The hard thresholding method generally has good denoising performance, but it may cause oscillations in the reconstructed ECG signal, known as the pseudo-Gibbs phenomenon, which limits its application [12]. Meanwhile, soft thresholding can produce a smoother ECG signal and has better continuity. However, soft thresholding distorts the amplitude of the reconstructed waveform, especially for the R wave amplitude in the QRS complex [13]. In the EMD-based denoising methods, the noise signal is decomposed into intrinsic mode functions (IMFs), and the IMF containing the most noise is removed, and the remaining IMFs are used to reconstruct the denoised

signal. The EMD method may not be able to clearly distinguish high-frequency noise and QRS waves, and cannot effectively separate similar frequency signals, resulting in the P wave and T wave in the ECG signal being filtered out, leading to misdiagnosis [14]. Filter-based algorithms have good denoising effects, but they can only filter out noise in an offline state and are prone to complex noise mixing during signal transmission, affecting the waveform. Common simple filtering methods cannot ensure effective noise removal while retaining complete ECG signal useful information.

With the development of deep learning, there are increasingly more deep learning-based noise reduction models for ECG signals. These deep learning-based models have achieved noise reduction effects as good as those of traditional methods, and even better. Wangg et al. [15] proposed a deep neural network (DNN) consisting of a denoising autoencoder (DAE) after wavelet transformation to eliminate noise from electrocardiogram (ECG) signals. They filtered most of the noise using wavelet transformation and a scale-adaptive threshold method, and then removed the residual noise using an improved neural network. However, they ignored the noise of baseline drift, which could be several times higher than the ECG signal itself. Lv [16] was the first to attempt to use deep learning based on the long short-term memory (LSTM) model to suppress noise in ECG signals. Using the transfer learning method, they pre-trained the network with synthetic data generated by the dynamic electrocardiogram model and fine-tuned the network with real data. They did not consider the influence of baseline drift on the signal, and this method is prone to overfitting. Zhang et al. [17] conducted the first research on using a denoising autoencoder (DAE) based on the fully convolutional network (FCN) to reduce noise in ECG signals. Compared with the denoising models based on DNN and CNN, FCN has better noise reduction performance under the same compression ratio. Although the existing noise reduction methods have achieved some results, there are still two problems: First, the noise signal in ECG is complex, and traditional noise reduction methods cannot accurately obtain the features of the noise and lose some useful ECG signals during denoising, resulting in the failure of cardiovascular disease diagnosis; Second, some noise signals and ECG signals have overlapping frequencies, and some noise has a significant impact on the waveform morphology of the tiny wave P wave and T wave, causing obvious waveform changes.

Based on this, in order to further improve the noise reduction effect of ECG signals that are overwhelmed by complex noise in the context of remote medical care, and to more accurately capture the waveform features of ECG signals, while avoiding the loss of ECG information during noise reduction, this paper proposes a heart signal noise reduction method based on the deep fully convolutional enhancement network (FCBN). Since the convolutional layer has local connectivity, each neuron only depends on a small area of the previous layer, replacing the final fully connected layer of CNN with the convolutional layer to obtain FCN. The receptive field of FCN is small, enabling FCN to effectively extract and preserve local information features. At the same time, the input signal features share the same weights in the receptive field, reducing the number of parameters and making the hardware implementation simpler. Then, the traditional manual enhancement unit in the Boosting algorithm is replaced by FCN, and multiple FCNs are integrated using the feedback method. Each individual FCN acts as a noise reduction module, and the filters of the convolutional layer in the FCN can extract waveform feature mappings to describe the characteristics of the input signal data [18-20]. Due to the overlap of ECG signals and noise, some signals may be lost during noise reduction, and the Boosting algorithm combines the output signal after each level of FCN noise reduction with the original input signal as the input data for the next independent network module for retraining of new model parameters, and gradually reduces noise. The original input signal data can be recovered in each independent noise reduction sub-module, and the waveform changes of the noise-reduced signal are smaller compared to the clean signal, and more signal morphological features are retained. Compared with other noise reduction methods, the noise reduction effect of this method is better, and the reconstructed ECG signal has less difference from the original clean signal, reducing the loss of ECG signals during noise reduction.

2. Proposed Method

This paper combines the GAN and Boosting algorithms to construct the GAN-Boosting network. The noise reduction method in this paper mainly consists of four parts: signal preprocessing, network initialization, training the GAN-Boosting noise reduction network [21,22], and reconstructing the noise-reduced signal. Firstly, the original electrocardiogram signals downloaded from the database are preprocessed, such as normalization and extraction of electrocardiogram samples. The weights of each layer of the network are initialized using the clean original signals. Then, the preprocessed sample data is input into each level of the GAN network for convolution layer processing. The filters in the convolution layer extract the signal features and eliminate the noise at the same time. The Boosting algorithm is used to stack multiple GAN networks to form a deep neural network. Due to the compression of the pooling layer on the features, the extracted ECG signal features will be lost. To better ensure the integrity of the signal, the pooling layer in the GAN network is cancelled. Finally, the signal is reconstructed through the deconvolution process.

2.1. GAN

GANs were proposed by Groodfellow et al. in 2014. It consists of two parts: the generator (G) and the discriminator (D). The task of the generator is to take randomly generated Gaussian noise as input and synthesize generated data. The task of the discriminator is to take real data and the generated data synthesized by the generator as input, and determine whether the current data is real or generated. The training process can be summarized by Equation (1).

$$\min_{G}\max_{D} V(G,D) = E_{x-P_{data(x)}}[\log D(x)] + E_{z-P_{z(z)}}[\log(1-D(G(z)))]. \tag{1}$$

Here, x represents the dataset, z is the input noise variable, and $G(z)$ is the data generated by the generator. $D()$ represents the probability that the discriminator judges the data to be true. GAN achieves the game process between the generator G and the discriminator D by optimizing the loss $V(G,D)$. The generator synthesizes to minimize the probability that the discriminator judges the generated data as false. Meanwhile, the discriminator needs to maximize the probability of judging the generated data as false and the real data as true. The adversarial generative model was proposed after its introduction and provided a new feasible method for the generation task. However, it also has problems such as unstable training, difficulty in convergence, and prone to mode collapse.

2.2. Boosting Algorithm

Boosting is a robust algorithm that improves the performance of different tasks by iteratively applying multiple controllable models. Yu et al. [23] proposed the earliest polynomial-time Boosting algorithm, but it was unable to be applied to practical problem research due to too many flaws. Zhang et al. [24] proposed the AdaBoost algorithm, which solved many practical problems of the earlier Boosting algorithms and gradually applied to various studies. For example, the image denoising model [25] enhances the denoised signal by extracting residual signals or eliminating noise residuals, iteratively enhancing the signal-to-noise ratio and improving the image reconstruction performance. Zhang et al. [26] proposed the Strengthen-Operate-Subtract (SOS) algorithm, which was an improvement of the Boosting algorithm. It combined the denoised image with the original input, iteratively improving the signal-to-noise ratio and achieving excellent improvement effects. Wang et al. [27] proposed the Deep Boosting framework (DBF), using the Dense Expansion Fusion Network (DDFN) as the embodiment of the enhancement unit, to achieve image denoising in the real world. This network solves the problem of gradient disappearance during the training process due to the excessively long network cascading, and simultaneously improves the efficiency of limited parameters.

Using the Boosting algorithm for noise reduction mainly aims to recover the clean signal $x(n)$ from the noisy signal sample $y(n)$. Assume $y(n) = x(n) + v(n)$, where $x(n)$ is the original clean electrocardiogram signal, and $v(n)$ is the noise signal. The noise reduction process is expressed as:

$$\hat{n} = S(y(n)) = S(x(x) + v(n)). \tag{2}$$

In the formula, $S()$ represents the noise reduction method. $\hat{x}(n)$ is the output signal after noise reduction. If the noise reduction effect is good, $\hat{x}(n)$ is an approximate value of $x(n)$.

In fact, $\hat{x}(n)$ is not equal to $x(n)$, and the difference between the two is:

$$u(n) = \hat{x}(n) - x(n) = v(n)_r - x(n)_r. \tag{3}$$

In the formula, $x(n)_r$ represents the original signal that was lost during the noise reduction process. $v(n)_r$ represents the noise signal that has not been removed.

A simple idea for applying the Boosting algorithm to signal denoising is to iteratively extract the unrecovered signal $x(n)$ from the residuals and add it back to the denoised signal $\hat{x}(n)$. After N iterations, we obtain:

$$\hat{x}(n)^{(N+1)} = \hat{x}(n)^{(N)} + H(y(n) - \hat{x}(n)^{(N)}). \tag{4}$$

In the formula, $H()$ represents the iterative process. Let $\hat{x}(n)^{(0)} = 0$. $y(n) - \hat{x}(n)$ not only includes the unrecovered signal $x(n)$, but also contains a part of the noise.

$$y(n) - \hat{x}(n) = x(n)_r + (v(n) - v(n)_r). \tag{5}$$

After noise reduction through iterative filtering, the signal $\hat{x}$ removes the remaining noise of u_r.

2.3. LSTM

As the network hierarchy deepens, the feature extraction process gradually shifts from a coarse-grained to a fine-grained approach, with the dimension of the feature map decreasing layer by layer, thereby capturing the characteristic information of different levels in the electrocardiogram signal. Finally, the feature map is compressed into a fixed size through the adaptive average pooling layer and transformed into a 512-dimensional feature vector through the flattening operation. By combining CNN and LSTM, the model can not only capture local features but also effectively handle temporal dependencies, thereby improving the analysis accuracy of complex time series signals.

The LSTM model, as an extension of RNN, has demonstrated its effectiveness in the field of sequential data based on its ability to solve the gradient vanishing problem that occurs in RNN when dealing with long-term dependent data. Importantly, LSTM achieves long-distance information transmission without losing the cell state information [28], as shown in Figure 1. Here, f_t, i_t, C_t, O_t represent the forget gate, input gate, cell state, and output gate respectively. The input sequence is denoted as x_t. The output of the previous unit block is represented as h_{t-1}. The state value of the previous storage block is represented by C_{t-1}. The state update process is marked by the symbol C'_t. The weight parameters and bias parameters are represented by W and b respectively. The input gate creates new R peak position information through the bias parameter, and the output gate generates the current R-peak position information of the electrocardiogram signal.

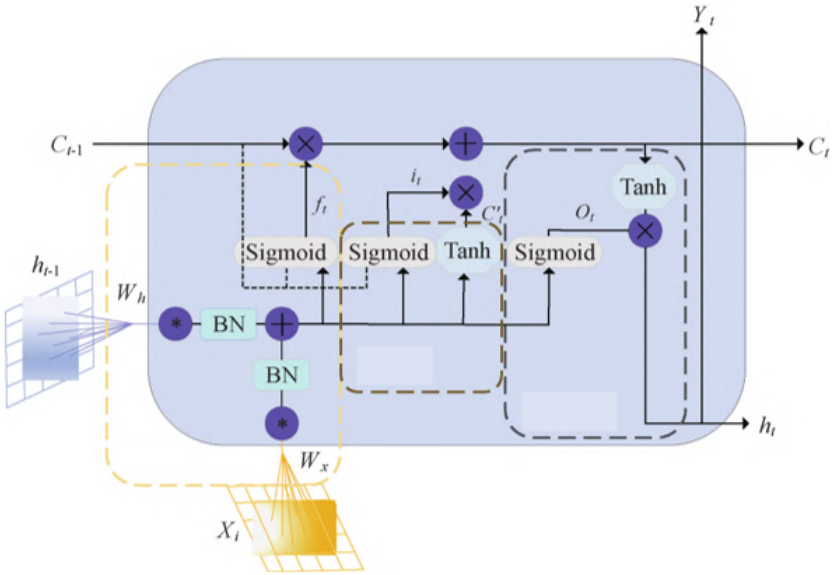

Fig. 1. LSTM structure

ResNet extracts image features from the data and converts them into 512-dimensional vector values. These vector values are then passed as input to the LSTM network, where an LSTM model with a single hidden layer is used to conduct in-depth time series analysis of the extracted features. Finally, through the Dropout and ReLU layers in the output layer, combined with a linear classifier, effective classification of the features is achieved. The schematic diagram of the ResNet-LSTM network is shown in Figure 2. The design of the hybrid model fully utilizes the advantages of ResNet in image feature extraction and the expertise of LSTM in handling time series data, thereby improving the accuracy of R-wave detection.

3. Experiments and Result Analysis

3.1. Experimental Data

The data used in this experiment were obtained from the clean electrocardiogram (ECG) signals in the MIT-BIH Arrhythmia Database [29]. This database contains 48 sets of dynamic ECG recordings sampled at 360 Hz, with each set having a data length of 30 minutes. The experiment selected 10 data points from the database (103, 105, 111, 116, 122, 205, 213, 219, 223, and 230) for presentation.

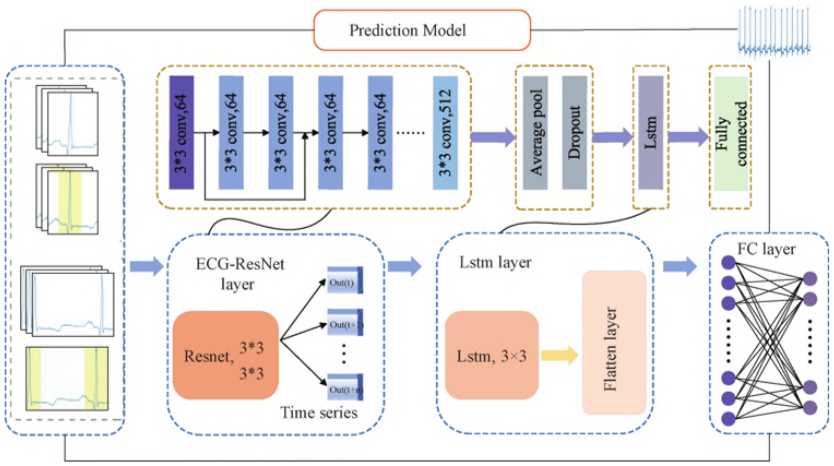

Fig. 2. ResNet-LSTM network

3.2. Data Preprocessing

In the experiment, all the signals were preprocessed first. The noisy ECG signals were superimposed onto the 48 groups of ECG signals in the arrhythmia database by three types of noise data, with the input signal-to-noise ratios being 1.25 dB and 5 dB. The input data samples in the network were selected based on the periodic characteristics of the electrocardiogram signals, and the appropriate length of electrocardiogram vectors were chosen. In this experiment, 300 segments were extracted from each data, with each segment consisting of 1024 sampling points as the sample input. A total of 14,400 segments were obtained, among which 80% formed the training set, 10% formed the validation set, and 10% formed the test set. The signal-to-noise ratios of the training set and the validation set were the same.

3.3. Evaluation Index

This paper uses two indicators, Signal-to-Noise Ratio (SNR) and Root Mean Square Error (RMSE), to evaluate the performance of the noise reduction algorithm [30].

If $x(n)$ represents the clean ECG signal, $\hat{x}(n)$ is the denoised ECG signal, and N is the length of the ECG signal, then the SNR is defined as:

$$SNR = 10\log\left(\frac{\sum_{i=1}^{N}(x(i))^2}{\sum_{i=1}^{N}(x(i)-\hat{x}(i))^2}\right). \tag{6}$$

The signal-to-noise ratio represents the ratio between the clean electrocardiogram signal and the noise. It is measured in decibels (dB) and is an important indicator for evaluating the quality of the signal. The higher the signal-to-noise ratio, the better the noise reduction effect of the signal.

Another indicator is the root mean square error. The root mean square error represents the difference between the denoised signal and the original true signal. The lower the root mean square error, the better the filtering performance for the signal. The definition of RMSE is:

$$RMSE = \sqrt{\frac{1}{N}\sum_{i=1}^{N}(x(i)-\hat{x}(i))^2}. \tag{7}$$

3.4. Experimental Results and Discussion

In order to verify that the noise reduction method proposed in this paper also has a good noise reduction effect on specific electrocardiogram (ECG) signals, the experimental results present the noise reduction results of adding 1.25 dB noise to the ECG signal No. 219 in the MIT-BIH database. Since the patient of data No. 219 suffers from paroxysmal atrial fibrillation, there are paroxysmal variable heartbeats in this data signal, and the RR interval (the interval between two R waves on the electrocardiogram) is irregular. Specific ECG signals often play a crucial role in doctors' correct diagnosis, but many ECG noise reduction methods cannot effectively reduce the noise of variable ECG signals. At the same time, the noise reduction methods proposed in this paper for three types of noise

(BM, MA, and EM) are compared with the noise reduction algorithms of wavelet threshold method (WTSub-band), S-transform method (S-Transform), BP neural network method (BPNN), and convolutional autoencoder (CAENN). Ten data from the database (103, 105, 111, 116, 122, 205, 213, 219, 223, and 230) are selected for presentation. In this experiment, the noise reduction network performs well in learning the specific features of the training signal and can retain the pathological information when filtering out the noise.

Baseline drift (BW) is the most common type of noise in electrocardiogram (ECG) signals, arising from the influence of human breathing on the heartbeats during the acquisition process. Figure 3 shows the denoised result of signal No. 219 with a 1.25 dB baseline drift (BW). The first waveform in Figure 3 represents the clean signal, the second waveform represents the signal after adding 1.25 dB baseline drift, and the third waveform represents the denoised waveform. Since the frequency of baseline drift occurs between 0.05 and 2 Hz, it is a low-frequency signal and may affect the waveform shapes of the ST segment and small waves such as P wave or T wave. From the waveform changes in the area of the dotted line box in Figure 3, it can be seen that baseline drift causes the baseline of the ECG signal waveform to deviate and the overall trend to change. In the first waveform, the dotted line box shows a downward ST segment, but after the interference of baseline drift, the ST segment undergoes significant changes, with an elevation. Changes in the ST segment can lead to misdiagnosis of other diseases. However, after denoising with the network model proposed in this paper, compared with the original signal, it can be seen that the denoised signal waveform returns to a normal baseline and the waveform shape is basically consistent with the original signal.

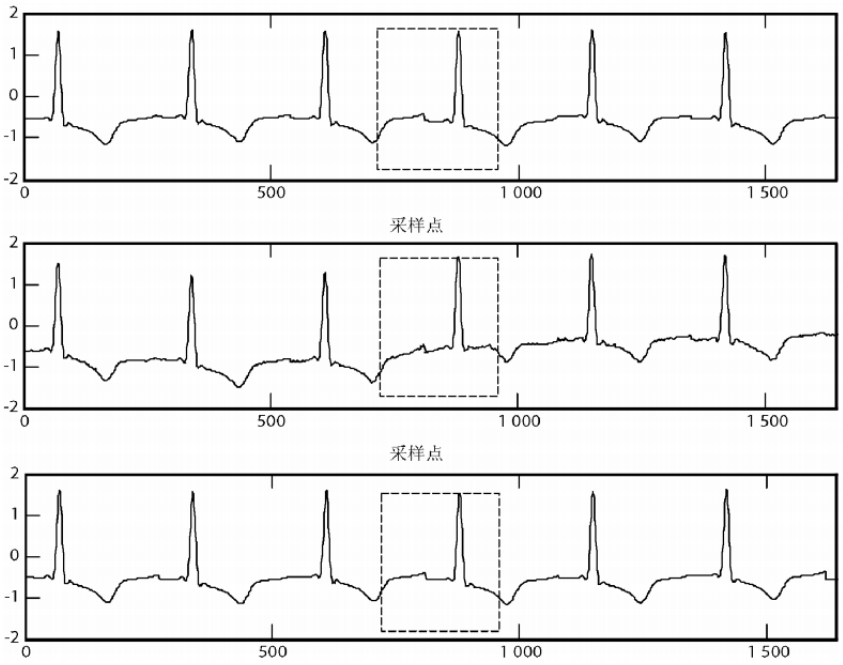

Fig. 3. The noise reduction result with eliminating a 1.25dB baseline drift

Table 1 shows the average results of the noise reduction methods proposed in this paper compared with the wavelet threshold method, S-transform method, BP neural network method and convolutional autoencoder noise reduction algorithm when filtering out 1.25 dB and 5 dB baseline drift noise for 10 data sets. The larger the SNR, the smaller the RMSE, and the closer the noise-reduced signal is to the original clean signal, with less distortion. From Table 1, it can be seen that the overall results of this method are better than those of the other four methods in terms of noise reduction effect. The SNR and RMSE have been significantly improved, indicating that the noise reduction method proposed in this paper has a better effect on filtering baseline drift noise in ECG signals.

Muscle electrical interference (MA) is caused by the contraction and expansion movements of the muscles. Figure 4 shows the noise reduction result of adding 1.25dB muscle electrical interference (MA) to signal No. 219. The muscle electrical interference noise is manifested as constantly changing small spikes in the signal, which belongs to high-frequency signals. Such noise can drown out the P wave and T wave of the electrocardiogram signal, causing the original shape to become blurred. Due to the overlap of the muscle electrical interference frequency with the ECG signal frequency, filtering out such noise often results in the loss of useful information in the ECG signal. From Figure 4, when 1.25dB muscle electrical interference noise is added, the waveform

Table 1. The experimental results of eliminating baseline drift

noise/dB	Index	WT	ST	BPNN	CAENN	Proposed
1.25	SNR	1.52	11.386	11.25	14.853	17.331
1.25	RMSE	0.838	0.273	0.143	0.095	0.059
5	SNR	5.307	12.672	12.007	15.832	18.858
5	RESM	0.542	0.273	0.114	0.082	0.047

shape of the low-frequency component signal in the ECG signal is submerged, causing the loss of low-frequency signals. The 219th ECG signal has the P wave disappear due to the occurrence of atrial fibrillation, but when the muscle electrical noise interference occurs, the waveform shape of the low-frequency signal undergoes severe changes, making it impossible to determine whether there is a P wave or T wave, and thus unable to diagnose the disease from the noisy signal. However, after noise reduction using the method in this paper, not only is the influence of muscle electrical interference noise eliminated, but also the low-frequency signal waveform shape is well preserved in some RR periods, retaining the pathological signal characteristics of the disappearance of the P wave in the original signal.

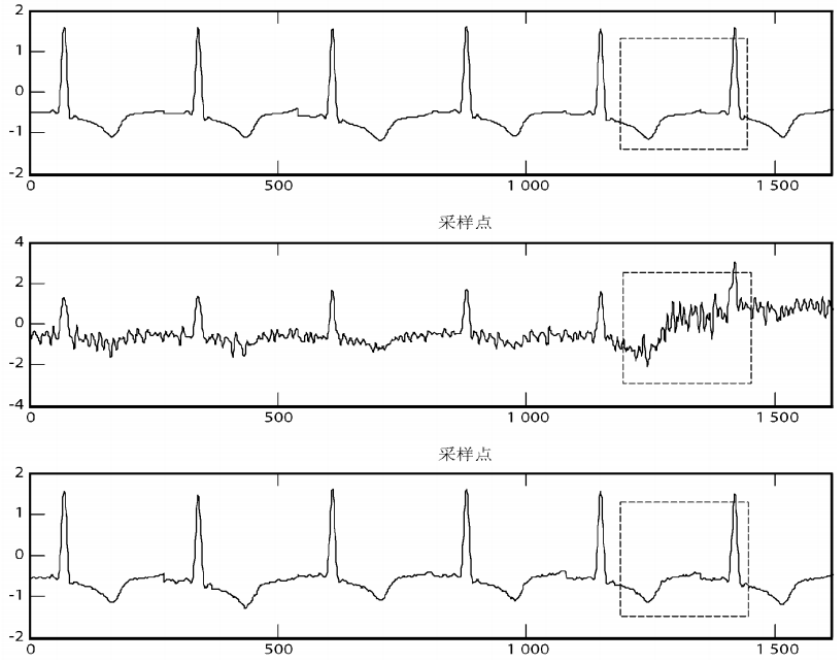

Fig. 4. The noise reduction result with filtering out 1.25dB of muscle electrical interference

Table 2 shows the comparison results of the proposed method with the wavelet threshold method, S-transform method, BP neural network method, and convolutional autoencoder denoising algorithm when filtering out 1.25dB and 5dB electromyographic interference noise from 10 data sets. It can be seen that in the noise reduction of ECG signals with 1.25 dB electromyographic interference, the denoising effect of the proposed method on data 230 is the most prominent. Overall, after denoising the ECG signals with 1.25dB electromyographic interference using WT-Subband, S-Transform, BPNN, and CAENN methods, the average SNR is 2.821, 9.660, 9.257, and 11.900 respectively, and the average RMSE is 0.730, 0.332, 0.181, and 0.134 respectively; after denoising with the algorithm proposed in this paper, the average SNR reaches 13.869, and the average RMSE value drops to 0.079.

Electrode interference (EM) is the noise generated by the electrode patches adhered to the skin. Figure 5 shows the noise reduction result of adding 1.25dB electrode interference to signal No. 219. It randomly generates step-like interference, which alters the amplitude profile and baseline position of the ECG. As can be seen from Figure 5, the amplitude of the electrode interference noise is smaller than that of the muscle electrical interference noise, and the addition of electrode interference alters the morphology of the low-frequency waves in the original ECG signal, but is very similar to the waveform amplitude in the original signal. This poses a challenge in filtering

Table 2. The experimental results after eliminating muscle electrical interference

noise/dB	Index	WT	ST	BPNN	CAENN	Proposed
1.25	SNR	2.821	9.66	9.257	11.9	13.869
1.25	RMSE	0.73	0.332	0.181	0.134	0.079
5	SNR	6.39	11.57	10.3	13.18	14.883
5	RESM	0.484	0.267	0.157	0.116	0.069

out the electrode interference noise while retaining the original low-frequency wave morphology. Especially for signal No. 219, which has variable heartbeats, the addition of electrode interference noise causes a waveform pattern similar to the P wave, confusing the pathological waveform characteristics of the variable heartbeats in the original signal. However, after being processed with the noise reduction method proposed in this paper, the electrode interference is well filtered out, and the waveform characteristics of the variable heartbeats are well preserved.

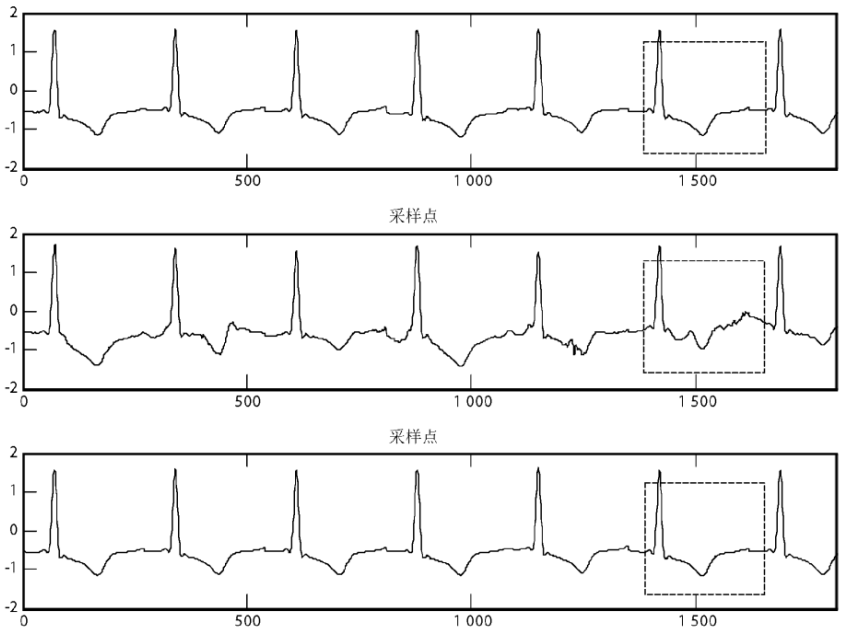

Fig. 5. The noise reduction result with filtering out 1.25dB of electrode interference

Table 3 shows the average results of SNR and RMSE when 1.25 dB and 5 dB electrode interference noise are filtered out for 10 data sets. By comparing with Table 2, it can be seen that the method proposed in this paper also has obvious advantages in filtering out electrode interference.

Table 3. Experimental results after eliminating electrode interference

noise/dB	Index	WT	ST	BPNN	CAENN	Proposed
1.25	SNR	1.641	7.013	9.34	14.227	16.316
1.25	RMSE	0.824	0.447	0.171	0.097	0.066
5	SNR	5.406	9.708	10.757	15.137	17.308
5	RESM	0.535	0.329	0.148	0.084	0.058

4. Conclusion

This paper studies and proposes a noise reduction method based on a deep fully convolutional enhancement network. By combining the Boosting algorithm with the GAN, it is used to filter out the complex noise in the

ECG signals collected by the equipment. Whether in terms of the changes in the waveform after noise reduction or through quantitative comparison with the noise reduction results of wavelet threshold method, S transform method, BP neural network method and convolutional autoencoder, the noise reduction method based on the deep GAN-Boosting network model outperforms the other four methods in terms of noise reduction and preservation of clinical details, and can achieve better noise reduction effects. At the same time, by using the SOS enhancement algorithm, by inputting the original noisy ECG signal in multiple levels, stacking multiple GAN networks, the depth of the network is increased, and the learning and capturing of the main waveform features of the electrocardiogram signal by the GAN network are enhanced. The features such as P wave and T wave are well preserved, avoiding the loss of useful ECG information during the noise filtering process. In conclusion, the noise reduction method proposed in this paper has good application value and practical significance in the preprocessing stage of intelligent diagnosis of cardiovascular diseases.

5. Conflict of Interest

The authors declare that there are no conflict of interests, we do not have any possible conflicts of interest.

Acknowledgments. This research was supported by the Henan Provincial Scientific and Technological Research Project (No.252102210005,222102310222)the Training Program for Young Backbone Teachers in Higher Education Institutions of Henan Province(No.2025GGJS149).

References

1. Joseph P, Lanas F, Roth G, et al. Cardiovascular disease in the Americas: the epidemiology of cardiovascular disease and its risk factors[J]. The Lancet Regional HealthCAmericas, 2025, 42.
2. Abdellatif M, Schmid S T, Fuerlinger A, et al. Anti-ageing interventions for the treatment of cardiovascular disease[J]. Cardiovascular Research, 2025, 121(10): 1524-1536.
3. Chong B, Jayabaskaran J, Jauhari S M, et al. Global burden of cardiovascular diseases: projections from 2025 to 2050[J]. European journal of preventive cardiology, 2025, 32(11): 1001-1015.
4. Yin S, Wang L, Chen T, et al. LKAFormer: A Lightweight Kolmogorov-Arnold Transformer Model for Image Semantic Segmentation[J]. ACM Transactions on Intelligent Systems and Technology, 2025. doi:10.1145/3759254.
5. Yin S, Li H, Laghari A A, et al. FLSN-MVO: Edge Computing and Privacy Protection Based on Federated Learning Siamese Network With Multi-Verse Optimization Algorithm for Industry 5.0[J]. IEEE Open Journal of the Communications Society, vol. 6, pp: 3443-3458, 2024. doi:10.1109/OJCOMS.2024.3520562.
6. Shoulin Yin, Hang Li, Lin Teng, Asif Ali Laghari, et al. Brain CT Image Classification Based on Mask RCNN and Attention Mechanism[J]. Scientific Reports, https://doi.org/10.1038/s41598-024-78566-1.
7. Baldazzi G, Corda M, Solinas G, et al. Wavelet-based algorithms for noninvasive fetal ECG post-processing: A methodological review[J]. Biomedical Signal Processing and Control, 2026, 111: 108350.
8. Das M, Sahana B C. Optimized orthogonal wavelet-based filtering method for electrocardiogram signal denoising[J]. Journal of The Institution of Engineers (India): Series B, 2025, 106(3): 965-978.
9. Yan D, Liu B, Wang Y, et al. Enhancing precision in dispersion measurements of chirped fiber Bragg gratings with wavelet-based denoising[J]. Optics Express, 2025, 33(20): 42282-42291.
10. Wnk A, Kudas D. Application of combination of denoising methods and Complementary Ensemble Empirical Mode Decomposition in GNSS time series analysis[J]. GPS Solutions, 2025, 29(3): 141.
11. Nair S, James B P, Leung M F. An optimized hybrid approach to denoising of EEG signals using CNN and LMS filtering[J]. Electronics, 2025, 14(6): 1193.
12. Zhang Y. Image Denoising Based On Deep Feature Fusion And U-Net Network[J]. Journal of Applied Science and Engineering, 2025, 28(10): 2277-2285.
13. Shen W. A novel conditional generative adversarial network based on graph attention network for moving image denoising[J]. Journal of Applied Science and Engineering, 2022, 26(6): 829-839.
14. Feng L, Li J, Zhang Y, et al. Deep-learning-driven Cross-modal Image Fusion For Cartoon Captioning[J]. Journal of Applied Science and Engineering, 29(5): 1203-1210.
15. Wang K, Xin W. The application of acoustic detection technology in the investigation of submarine pipelines[J]. Journal of Applied Science and Engineering, 2024, 27(8): 2981-2991.
16. Lv H. A Hybrid Computational Framework For Enhance Wind Power Forecasting Using Improved Akima-Empirical Mode Decomposition And Deep Neural Networks In Smart Grid Applications[J]. Journal of Applied Science and Engineering, 29(6): 1307-1322.
17. Zhang Y, Lin R, Zhao L. A Time Compensation Based Algorithm For Predicting Surface Defects In Iron Ore Sintering[J]. Journal of Applied Science and Engineering, 2024, 27(12): 3761-3768).
18. Yu J, Lu Z, Yin S, et al. News recommendation model based on encoder graph neural network and bat optimization in online social multimedia art education[J]. Computer Science and Information Systems, vol. 21, no. 3, pp. 989-1012, 2024. doi: 10.2298/CSIS231225025Y.

19. Yin S, Li H, Laghari A A, et al. An anomaly detection model based on deep auto-encoder and capsule graph convolution via sparrow search algorithm in 6G internet-of-everything[J]. IEEE Internet of Things Journal, vol. 11, no. 18, pp. 29402-29411, 2024. DOI: 10.1109/JIOT.2024.3353337.
20. Laghari A A, Li H, Shoulin Y, et al. Blockchain applications for Internet of Things (IoT): A review[J]. Multiagent and Grid Systems, 2023, 19(4): 363-379.
21. Zhang S, Zou C, Yap S P, et al. Generative adversarial network-enhanced machine learning models for high-precision prediction of rectangular concrete-filled steel tube strength[J]. Engineering Structures, 2025, 339: 120514.
22. Gaur P, Gowda D, Kumari S, et al. Deep Learning-Driven Facial Emotion Recognition with GANs for Optimizing Student Learning[C]//2025 3rd International Conference on Sustainable Computing and Data Communication Systems (ICSCDS). IEEE, 2025: 1610-1617.
23. Yu T, Zhong X, Guan Y. Polynomial-Time Algorithms for Deterministic Uncapacitated Lot-Sizing Problem with Heterogeneous Production Cycles[J]. Operations Research Letters, 2025: 107304.
24. Zhang X, Yu L, Yin H. An Ensemble Resampling Based Transfer AdaBoost Algorithm for Small Sample Credit Classification with Class Imbalance[J]. Computational Economics, 2025, 65(6).
25. Jiang, Y., Yin, S. Heterogenous-view Occluded Expression Data Recognition Based on Cycle-Consistent Adversarial Network and K-SVD Dictionary Learning Under Intelligent Cooperative Robot Environment[J]. Computer Science and Information Systems, vol. 20, no. 4, pp. 1869-1883, 2023.
26. Zhang Y, Jia Y, Zhou Q, et al. AR-MANet: A Low-Quality Image Restoration Method Based on Multi-Feature Fusion[J]. IEEE Signal Processing Letters, 2025.
27. Wang X, Luo Z, Huang W, et al. Optimized UNet framework with a joint loss function for underwater image enhancement[J]. Scientific Reports, 2025, 15(1): 7327.
28. S. Yin, L. Wang, M. Shafiq, L. Teng, A. A. Laghari and M. F. Khan, "G2Grad-CAMRL: An Object Detection and Interpretation Model Based on Gradient-Weighted Class Activation Mapping and Reinforcement Learning in Remote Sensing Images," in IEEE Journal of Selected Topics in Applied Earth Observations and Remote Sensing, vol. 16, pp. 3583-3598, 2023, doi: 10.1109/JSTARS.2023.3241405.
29. AIT BOURKHA M E, HATIM A, NASIR D, et al. Optimized wavelet scattering network and cnn for ecg heartbeat classification from mitCbih arrhythmia database[J]. International Journal of Advanced Computer Science & Applications, 2025, 16(2).
30. Shoulin Yin, Hang Li, Desheng Liu and Shahid Karim. Active Contour Modal Based on Density-oriented BIRCH Clustering Method for Medical Image Segmentation [J]. Multimedia Tools and Applications. Vol. 79, pp. 31049-31068, 2020.